FULL PAPER

Dalton
www.rsc.org/dalton

Palladium(II)-based *cis*,*trans*-1,3,5-triaminocyclohexane complexes demonstrating a variety of coordination modes and architectures †

Georg Seeber,[a] De-Liang Long,[a] Benson M. Kariuki[b] and Leroy Cronin*[a]

[a] *Department of Chemistry, The University of Glasgow, University Avenue, Glasgow, UK G12 8QQ. E-mail: L.Cronin@chem.gla.ac.uk; Fax: +44 141 330 4888; Tel: +44 141 330 6650*

[b] *School of Chemical Sciences, The University of Birmingham, Edgbaston, Birmingham, UK B15 2TT*

Received 3rd July 2003, Accepted 5th September 2003
First published as an Advance Article on the web 3rd October 2003

The reaction of *cis*,*trans*-1,3,5-triaminocyclohexane·3HX (**L**·3HX) with PdX_2 (X = Br, Cl) affords a wide range of coordination complexes that represent the different coordination modes available to **L**. Monoligand complexes $[Pd(\mathbf{L}H)Cl_2]Cl$ (**1**) and $[Pd(\mathbf{L}H)Br_2]_2[PdBr_4]$ (**2**) demonstrate the bidentate coordination of **L** with the two *cis* amino 'head' groups chelating the palladium(II) ion and the third *trans* amino 'tail' group being protonated. Diligand complexes $[Pd(\mathbf{L}H)_2]X$ (X = $(NO_3)_4$ **3**, $(SO_4)_2$ **4**) show a 'head-to-head' coordination mode with the protonated *trans* amino groups adopting a conformation that positions them opposite to each other. Both sets of amino groups are engaged in coordination in a cyclic 'head-to-tail' fashion found in the hexanuclear ring clusters $[\{Pd(\mathbf{L})X\}_6]X_6$ (X = Cl **5**, Br **6**). **5** and **6** are isostructural, both in the solid state and in solution, despite accommodating six chloro or bromo ligands into the cluster framework. A trinuclear complex $[Pd\{Pd(\mathbf{L})Cl_2\}_2Cl_2]$ (**7**) reveals 'tail-to-tail' coordination of two ligands for the centre palladium(II) ion in addition to their 'head' amino groups individually chelating other palladium(II) ions. Complexes **1**–**7** were characterised by single-crystal X-ray diffraction, elemental analysis, IR and by NMR spectroscopy (**1**–**6**).

Introduction

The self-assembly of metal-based coordination compounds provides a versatile approach to molecular architectures. Serendipitous approaches allow the discovery of systems that are not amenable to initial design as shown by the work of Winpenny and others.[1] However, examples of rationally designed building blocks are given by the groups of Raymond,[2,3] Lehn[4,5] and Saalfrank,[6,7] who take advantage of directed multibranched chelating ligands that show increased preorganization and high formation constants.[8] There are many splendid examples of rigid, highly directional multibranched monodentate ligands which bind to coordinatively unsaturated transition-metal complexes;[9–13] exemplified by the work of the groups of Fujita[9,14] and Stang.[15,16] Such structures include two-dimensional polygons as well as three-dimensional architectures such as truncated tetrahedra, dodecahedra and a wide variety of other systems.[9,15–18] It should be noted that the programmed self-assembly of such architectures can be achieved by choosing metal ions such as Pd(II) and Pt(II) with a number of the square-planar coordination sites 'blocked' by predominantly multidentate ancillary ligands.[19] This is because both Pd(II) and Pt(II) form inert complexes with chelating ligands while retaining sufficient lability with monodentate ligands to facilitate self-assembly of the overall architecture.[9,15] As a possible extension to this approach, current interest focuses on adopting self-assembly processes which overcome the need for ancillary ligands by using multiple, non-interacting and non-equivalent binding sites present in a single molecule.[20–22] In this respect, we have designed a set of ligands based upon *cis*,*trans*-trisubstituted-cyclohexane that provide two non-equivalent (bidentate 'head', monodentate 'tail') and non-interacting (*cis*,*trans*) coordination sites. We have recently reported the self assembly of a hexanuclear metallamacrocycle[22] as the first example of a structurally characterised complex based on the ligand *cis*,*trans*-1,3,5-triaminocyclohexane (**L** or *trans*-tach). Herein we extend our initial studies, demonstrating the versatility of this ligand as a new building block in the construction of supramolecular architectures.

Results and discussion

The lowest energy conformation of the uncomplexed ligand *trans*-tach (**L**) ligand shows the *cis*-amino groups in an equatorial, and the third *trans* amine in an axial, position with respect to the rigid cyclohexane backbone (Fig. 1, Top-left).

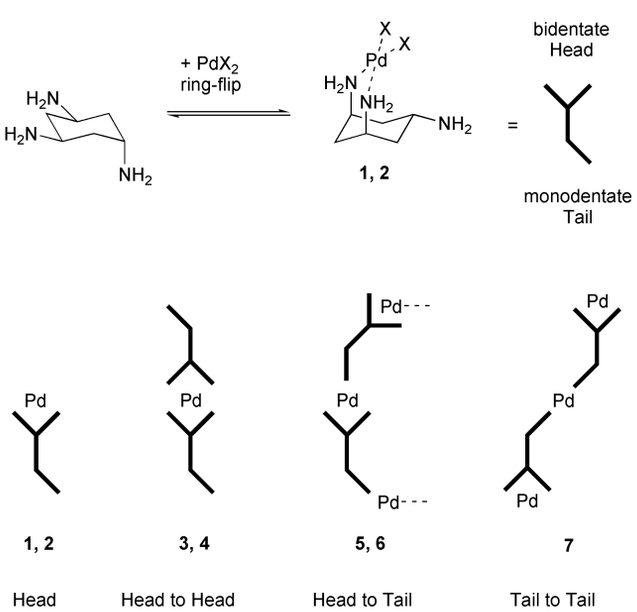

Fig. 1 Top-left: Tris-monodentate conformation. Top-right: Ring-flip to chelating 'head' and monodentate 'tail' conformation upon Pd(II) coordination. Bottom: Various coordination modes of *trans*-tach with Pd(II); remaining coordination sites are occupied by halide ligands: 'head' **1**, **2**; 'head-to-head' **3**, **4**; 'head-to-tail' **5**, **6**; 'tail-to-tail' **7**.

† Electronic supplementary information (ESI) available: A detailed description of the coordinative flexibility of *trans*-tach. Fig. S1: Diagram defining interplanar angle Θ and torsion angle χ. Table S1: interplanar angles Θ and torsion angles χ for complexes **1**–**7**. See http://www.rsc.org/suppdata/dt/b3/b307616d/

DOI: 10.1039/b307616d

Upon ring-flip, the two *cis* amino groups provide an axial bidentate chelating moiety ('head') which is suitable to form stable metal complexes and the *trans* amino group provides an equatorial monodentate coordination site ('tail', Fig. 1, Top-right). As such, the rigidity of the cyclohexane backbone ensures that the binding sites are non-interacting and therefore a number of different coordination modes is possible upon complexation to square-planar Pd(II) centres. For instance, the monoligand complexes [Pd(**L**H)Cl_2]Cl (**1**) and [Pd(**L**H)Br_2]$_2$-[$PdBr_4$] (**2**) (Fig. 1, Top-right) are obtained with two *cis* sites occupied by the 'head' chelation of **L** and the two remaining sites occupied by halide ligands. Coordination of a second *trans*-tach ligand can either occur *via* a second 'head' chelation ('head-to-head' complexes [Pd(**L**H)$_2$]X, X = $(NO_3)_4$ **3**, $(SO_4)_2$ **4**) or *via* 'tail' coordination of its *trans* amino group ('head-to-tail' complexes [{Pd(**L**)X}$_6$]X_6 (X = Cl **5** and Br **6**). A further coordination mode is observed in the trinuclear complex [Pd-{Pd(**L**)Cl_2}$_2$$Cl_2$] (**7**), where the centre Pd(II) ion is ligated by a 'tail-to-tail' coordination of two *trans*-tach ligands in addition to their 'head' amino groups individually chelating other Pd(II) ions (for crystallographic data see Table 1, for selected bond lengths and angles see Table 2).

A noteworthy measure of the ability of the ligand to accommodate strained coordination environments is the compressibility of the six membered metallacycle formed upon 'head' chelation (Fig. 1, Top-right). The more regular the metallacyclic chair conformation is, the more the Pd(II) is orientated towards the cyclohexane centre, resulting in an overall compressed structure. This coordinative flexibility is exemplified by variation in the compressed conformations observed in the solid-state structures of **1**–**7**.

'Head' coordination – monoligand complexes 1 and 2

Reactions of *trans*-tach trihydrochloride or -bromide salt with one equivalent of the corresponding palladium(II) halide produces the monoligand complexes [Pd(**L**H)Cl_2]Cl (**1**) or [Pd-(**L**H)Br_2]$_2$[$PdBr_4$] (**2**). In both complexes, the cyclohexane rings adopt a chair conformation with the 'head' amino groups involved in coordination to the Pd(II) ions and the square-planar coordination spheres are completed by two chloro (**1**) or bromo (**2**) ligands (Fig. 2), respectively. The remaining 'tail' amino groups are protonated and complexes **1** and **2** crystallise as chloride (**1**) or tetrabromopalladate (**2**) salts. The Pd–N and Pd–X bonds lie within expected ranges for square-planar *cis*-diamino-dichloro, and -dibromo palladium(II) complexes.[23–26]

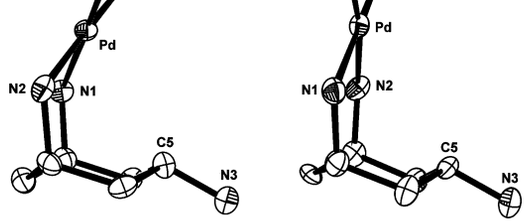

Fig. 2 ORTEP-3 representations of the monoligand cations of [Pd(**L**H)Cl_2]Cl (**1**, LHS) and [Pd(**L**H)Br_2]$_2$[$PdBr_4$] (**2**, RHS) at 50% thermal ellipsoids. Counterions and solvent molecules are omitted. The more compressed conformation of **1** can be seen clearly.

Geometrically, the position of the Pd(II) ions in complexes **1** and **2** differ in their orientation with respect to the cyclohexane ring resulting in a more compressed structure for **1**. Contrary to this, the Pd(II) coordination in complex **2** results in a distorted chair conformation for the six-membered metallacycle, placing the Pd(II) towards the edge of the cyclohexane ring. However, in contrast NMR studies show that the structures of **1** and **2** are

Table 1 Crystallographic data for complexes **1**–**4**, **6** and **7**

	[Pd(**L**H)Cl_2]Cl·H_2O **1**·H_2O	[Pd(**L**H)Br_2]$_2$[$PdBr_4$]·2H_2O **2**·2H_2O	[Pd(**L**H)$_2$]$(NO_3)_4$ **3**	[Pd(**L**H)$_2$]$(SO_4)_2$·6H_2O **4**·6H_2O	[{Pd(**L**)Br_6}]Br_6·20H_2O **6**·20H_2O	[Pd{Pd(**L**)Cl_2}$_2$$Cl_2$] **7**
Formula	$C_6H_{18}Cl_3N_3OPd$	$C_{12}H_{36}Br_8N_6O_2Pd_3$	$C_{12}H_{32}N_{10}O_{12}Pd$	$C_{12}H_{44}N_6O_{14}PdS_2$	$C_{36}H_{130}Br_{12}N_{18}O_{20}Pd_6$	$C_{12}H_{30}Cl_6N_6Pd_3$
M_r	360.98	1254.95	614.88	667.05	2732.90	790.32
T/K	298(2)	150(2)	298(2)	120(2)	120(2)	298(2)
Crystal system	Orthorhombic	Triclinic	Monoclinic	Monoclinic	Monoclinic	Monoclinic
Space group	$Pbc2_1$	$P\bar{1}$	$P2_1/c$	$P2_1/n$	$P2_1/n$	$I2/a$
a/Å	12.4445(1)	8.8314(4)	8.3934(11)	8.2588(2)	12.4054(2)	15.5544(9)
b/Å	12.2051(1)	8.8782(3)	16.6490(20)	17.3414(4)	26.6675(5)	9.6173(5)
c/Å	8.3213(1)	11.5103(6)	8.6914(11)	9.1518(2)	12.8312(2)	17.1240(9)
α/°	90	69.095(2)	90	90	90	90
β/°	90	76.249(2)	109.419(4)	99.120(1)	90.701(1)	90.0(4)
γ/°	90	60.895(2)	90	90	90	90
V/Å^3	1263.89(0)	734.35(11)	1145.46(17)	1294.14(2)	4244.51(12)	2561.6(2)
Z	4	1	2	2	2	4
F(000)	719.9	583.9	631.9	695.9	2655.6	1535.8
D_c/g cm^{-3}	1.90	2.838	1.78	1.712	2.138	2.05
μ/mm^{-1}	17.500	12.722	0.891	0.952	6.958	22.670
Reflections collected	5508	18770	6093	23350	26763	5038
Reflections unique	1904	3371	2026	5618	8317	2140
Cryst. det. distance/mm	40	40	80	40	40	40
$R1$[a]	0.046	0.045	0.085	0.036	0.041	0.086
$wR2$[b] (all data)	0.122	0.119	0.123	0.097	0.101	0.235

[a] $R1 = \Sigma(|F_o| - |F_c|)/\Sigma|F_o|$. [b] $wR2 = [\Sigma(w(F_o^2 - F_c^2)^2)/\Sigma(w(F_o^2)^2)]^{1/2}$.

Table 2 Selected bond lengths (Å) and angles (°) for **1**–**7**

[Pd(**L**H)Cl_2]Cl **1**	[Pd(**L**H)Br_2]$_2$[$PdBr_4$] **2**	[Pd(**L**H)$_2$]$(NO_3)_4$ **3**	[Pd(**L**H)$_2$]$(SO_4)_2$ **4**	[{Pd(**L**)Cl}$_6$]Cl_6 **5**	[{Pd(**L**)Br}$_6$]Br_6 **6**	[Pd{Pd(**L**)Cl_2}$_2$$Cl_2$] **7**
Pd–N	*Pd–N*	*Pd–N*	*Pd–N*	*Pd–N*	*Pd–N*	*Pd–N*
Head	*Head*	*Head*	*Head*	*Head*	*Head*	*Head*
Pd–N1 2.041(7)	Pd1–N1 2.036(6)	Pd–N1 2.054(6)	Pd–N1 2.063(2)	2.034(6)–2.063(5)	2.040(5)–2.077(5)	Pd1–N1 2.042(11)
Pd–N2 2.038(7)	Pd1–N2 2.062(6)	Pd–N2 2.053(6)	Pd–N2 2.055(2)			Pd1–N2 2.061(10)
				Tail	*Tail*	*Tail*
				Pd1–N6 2.063(5)	Pd1–N9 2.066(5)	Pd2–N3 2.063(12)
				Pd2–N3 2.072(5)	Pd2–N3 2.061(5)	
				Pd3–N9[b] 2.067(5)	Pd3–N6[b] 2.058(5)	
Pd–Cl	*Pd–Br*			*Pd–Cl*	*Pd–Br*	*Pd–Cl*
Pd–Cl1 2.325(2)	Pd1–Br1 2.4319(8)			Pd1–Cl1 2.292(2)	Pd1–Br1 2.4430(8)	Pd1–Cl1 2.325(3)
Pd–Cl2 2.317(2)	Pd1–Br2 2.4404(7)			Pd2–Cl2 2.316(2)	Pd2–Br2 2.4238(8)	Pd1–Cl2 2.318(3)
				Pd3–Cl3 2.308(2)	Pd3–Br3 2.4263(8)	Pd2–Cl3 2.302(3)
cis Cl–Pd–Cl	*cis Br–Pd–Br*	*cis N–Pd–N*	*cis N–Pd–N*	*cis N–Pd–Cl*	*cis N–Pd–Br*	*Cl–Pd–Cl*
Cl1–Pd–Cl2 92.6(1)	Br1–Pd1–Br2 92.1(3)	N1–Pd–N2 89.5(2)	N1–Pd–N2 94.79(6)	86.9(2)–91.4(2)	88.2(2)–91.6(2)	Cl1–Pd1–Cl2 93.9(1)
		N1–Pd–N2[a] 90.5(2)	N1–Pd–N2[a] 85.2(6)			Cl3–Pd2–Cl3[c] 177.3(2)
cis N–Pd–Cl	*cis N–Pd–Br*			*cis N–Pd–N*	*cis N–Pd–N*	
N1–Pd–Cl2 88.1(2)	N1–Pd1–Br2 85.73(2)	*trans N–Pd–N*	*trans N–Pd–N*	91.1(2)–92.9(3)	89.4(2)–92.1(2)	*cis N–Pd–N*
N2–Pd–Cl1 88.2(2)	N2–Pd1–Br1 87.7(2)	N1–Pd–N1[a] 180.0(3)	N1–Pd–N1[a] 180.0(1)			86.6(3)–90.5(3)
				trans N–Pd–N	*trans N–Pd–N*	
cis N–Pd–N	*cis N–Pd–N*			175.7(2)–177.3(2)	174.7(2)–177.7(2)	*N–Pd–N*
N1–Pd–N2 91.1(2)	N1–Pd1–N2 94.7(2)					N1–Pd1–N2 91.4(4)
						N3–Pd–N3[c] 177.8(6)

Symmetry codes: [a] = $-x, -y, -z$. [b] = $-x + 1, -y + 2, -z + 1$. [c] = $-x + 3/2, y, -z$.

similar in solution and this is indicated by the ^{1}H NMR shifts for the axial methine protons on C5 in both complexes **1** and **2** which give rise to low field shifted signals with δ 6.22 and 6.20 ppm, respectively. This is presumably due to the presence of the two coordinating halide ligands increasing the deshielding effect.[22,27,28]

'Head-to-head' coordination – *anti*-diligand complexes 3 and 4

Adsorption of **1** onto a strongly alkaline ion exchange resin causes the hydrolysis of the chloro ligands and subsequent neutralisation with nitric acid results in the formation of the 'head-to-head' complex $[Pd(\mathbf{L}H)_2](NO_3)_4$ (**3**, Fig. 3, LHS), in which the *trans*-tach ligands are orientated *anti* to each other. An alternative route can be taken by the reaction of *trans*-tach with palladium(II) nitrate by directly replacing the labile nitrato groups with two *trans*-tach ligands rather than *via* an isolated mono-ligand intermediate. In each case, the two 'tail' amino residues are protonated and the complex crystallises as its tetrakis-nitrate salt. The Pd–N bonds lie within expected ranges for square-planar tetraamino palladium(II) complexes.[29] The Pd(II) ion is centred with respect to the cyclohexane rings (Fig. 3, LHS).

The identical *anti*-diligand coordination isomer $[Pd(\mathbf{L}H)_2](SO_4)_2$ (**4**, Fig. 3, RHS) is obtained by reaction of *trans*-tach with palladium(II) sulfate. As in the reaction with palladium(II) nitrate, no intermediate mono-ligand complex was observed and both 'tail' amino residues are protonated and the complex crystallises as its *bis*-sulfate salt. The Pd–N bonds lie within expected ranges for square-planar tetraamino palladium(II) complexes.[29] Interestingly, comparison of the crystal packing of both complexes reveals that the singly negative charged nitrate counterions in **3** (Fig. 4, LHS) enable a denser packing of the $[Pd(\mathbf{L}H)_2]^{4+}$ tetracations within the crystal lattice than the doubly negative charged sulfate ions in **4** (Fig. 4, RHS), where additional water molecules are incorporated into the lattice. In solution, the axial methine protons on C5, C5* in complexes **3** and **4** show ^{1}H NMR shifts with δ 5.38 and 5.36 ppm, respectively. These are less deshielded compared to those in the mono-ligand complexes **1** and **2**, presumably due to the lack of halide ligands at the Pd(II) centre. Furthermore, the comparison of the chemical shifts suggests that unlike in the solid state, both cations of **3** and **4** adopt similar structures in solution.

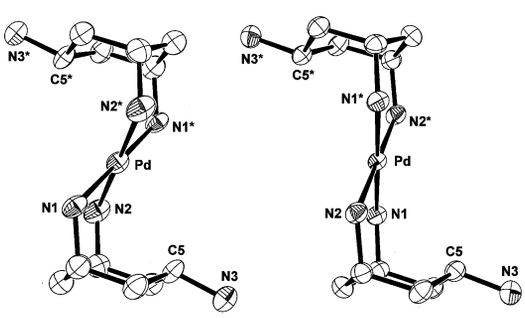

Fig. 3 ORTEP-3 representations of the *anti*-diligand cations of $[Pd(\mathbf{L}H)_2](NO_3)_4$ (**3**, LHS) and $[Pd(\mathbf{L}H)_2](SO_4)_2$ (**4**, RHS) at 50% thermal ellipsoids. Counterions and solvent molecules are omitted. The compressed conformation of **3** can be seen clearly. Both the Pd centres rest on crystallographic inversion centres.

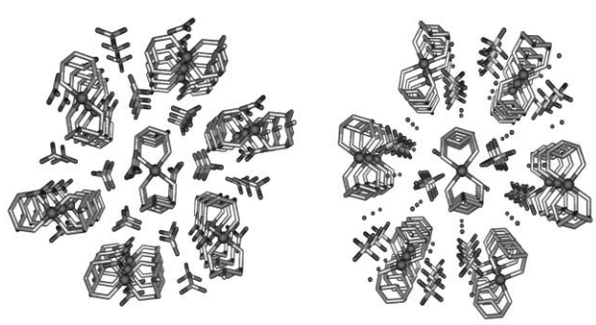

Fig. 4 Crystal packing of *anti*-diligand complexes **3** (LHS) and **4** (RHS) along the crystallographic *a* axis. Pd(II) centres are shown as large spheres, water molecules as small spheres. Trigonal planar and tetrahedral ions are nitrate and perchlorate counterions, respectively.

'Head-to-tail' coordination – hexanuclear ring structures 5 and 6

We have previously reported[22] the formation of the cyclic hexanuclear Pd(II) complex $[\{Pd(\mathbf{L})Cl\}_6]Cl_6$ (**5**) from the neutralisation of a solution of **1**. Identical reaction conditions applied to a solution of complex **2** result in the formation of the hexanuclear metallamacrocyle $[\{Pd(\mathbf{L})Br\}_6]Br_6$ (**6**). This complex is a bromo-substituted analogue of **5**, despite the sterically constrained cavity present in both metallamacrocycles. Before neutralisation, the tetrabromopalladate counterions were ion exchanged to bromide anions, preventing competing nucleophilic reactions. In addition, applying a solution of **1** to a chloride ion exchange resin before neutralisation increases the previously reported yield for **5** from 30 up to 65%. This indicates the presence of interfering palladate counterions in the mother-liquor of **1** upon formation of **5** by alternative nucleophilic substitution pathways. Our proposed mechanism for the formation of the hexanuclear metallamacrocyles **5** and **6** starts with the deprotonation of the protonated 'tail' amino moieties of **1** and **2**. Thus, the resulting nucleophilic complexes can react with each other by substitution of one chloro (**1**) or bromo (**2**) ligand from a second moiety of **1** and **2**, respectively, leading to the 'head-to-tail' coordination of the resulting cyclic structures **5** and **6** (Fig. 5). High dilution and elevated reaction temperatures facilitate the formation of the discrete ring structures rather than the formation of oligo- or polymeric units.[15]

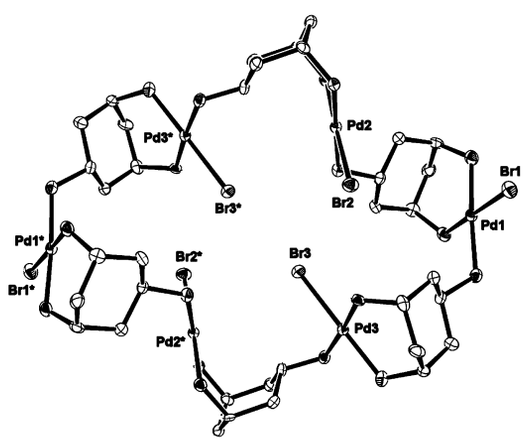

Fig. 5 ORTEP-3 representation of the cyclic cation of $[\{Pd(\mathbf{L})Br\}_6]Br_6$ (**6**) at 50% thermal ellipsoids. Counterions and solvent molecules are omitted.

The examination of the structures of **5** and **6** show that each Pd(II) is chelated by a 'head' amino group of one *trans*-tach ligand and by a monodentate 'tail' coordination of an adjacent ligand. With this 'head-to-tail' coordination, *trans*-tach acts both as a bridging ligand and as a corner unit, overcoming the need for ancillary ligands to complete the metallamacrocyclic arrangement. The square-planar coordination sphere is completed by a chloro (**5**) or bromo (**6**) ligand.

Both complexes comprise three crystallographically independent ring units‡ $\{Pd(\mathbf{L})X\}$ (X = Cl (**5**), Br (**6**)). A crystallographic inversion centre lies between the two coordinated halide

‡ Ring units 1, 2, 3 correspond to 'head' coordinating Pd1, Pd2, Pd3 cyclohexane rings, respectively. The cyclic complexes are formed by connection of each ring unit *via* their 'tail' amino group coordinating to a Pd(II) ion which is chelated by the 'head' amino group of an adjacent ring. Connectivity as follows: ring1–ring2–ring2–ring3–ring3–ring1.

ligands that point towards the centre of the cavity (X3 and X3*; Cl3 ··· Cl3* = 3.51 Å, Br3 ··· Br3* = 3.50 Å). In both complexes the six Pd(II) ions adopt a pseudo-chair conformation with the closest Pd2 ··· Pd3 distances being 5.19 and 5.10 Å and the furthest Pd1 ··· Pd1* distances being 13.72 and 13.76 Å for **5** and **6**, respectively. The three crystallographically independent Pd(II) centres exhibit different compressions towards their chelating cyclohexane rings. The similarity of the two complexes appears remarkable; a direct comparison by overlaying the weight centres§ of the heavy atoms of both crystal structures shows only slight deviations from one another (Fig. 6): the greatest deviations are 0.39 and 0.64 Å for Pd3 and X1, respectively.

The stability and rigidity of the hexanuclear ring clusters **5** and **6** are illustrated by their consistent NMR spectra in solution, ranging from room temperature up to 65 °C without change. A comparison between the ^{1}H NMR spectra of **5** and **6** is shown in Fig. 7. It is notable that differences in chemical shifts arise from the exchange of chloro (**5**) to bromo (**6**) ligands, whether due to the nature of the coordinating halides or due to solvent interactions. However, key features due to the structural restrictions of the metallamacrocyles are identical. The inversion centre present in both structures is maintained in solution and therefore three independent *trans*-tach environments are observed. Of particular interest are the most low field shifted signals H_A, H_B, H_C. Each of these axial methine protons represent one of the three independent ring units, integrating to one of the total number of 27 CH_n (n = 1, 2) protons in the asymmetric unit. The remaining protons are grouped into three sets of signals. Additionally, one isolated resonance for the axial methylene proton H_D is observed, which exhibits a *trans* coupling to H_B.

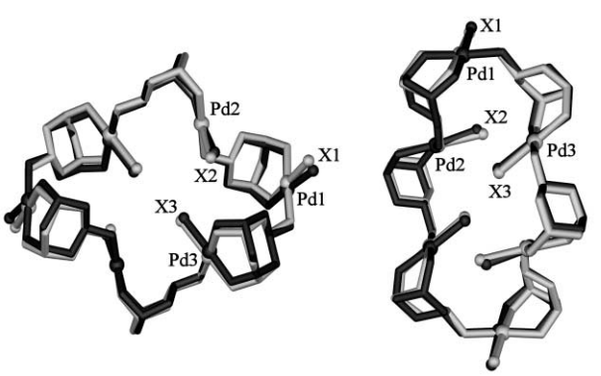

Fig. 6 Two views of the overlay of the weight centres of the heavy atoms in the cyclic cations **5** (Cl, black) and **6** (Br, grey). The Pd(II) centres deviate in distances 0.15, 0.33 and 0.39 Å for Pd2, Pd1 and Pd3, respectively, and the halide centres deviate in distances 0.25, 0.36 and 0.64 Å for X3, X2 and X1, respectively.

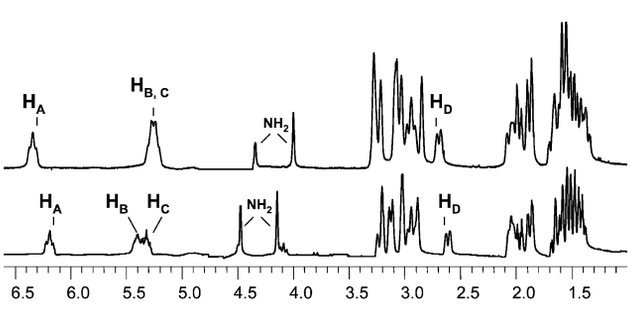

Fig. 7 ^{1}H NMR (400 MHz, D_2O) spectra of chloro- (**5**, Bottom) and bromo- (**6**, Top) metallamacrocycles.

§ The centroids of the six palladium(II) ions in the clusters were overlayed and the centroid distances of each set of crystallographically independent palladium(II) ions were minimised.

'Tail-to-tail' coordination – trinuclear complex 7

The 'tail-to-tail' coordination mode is observed in the trinuclear complex [Pd{Pd(**L**)Cl_2}$_2$$Cl_2$] (**7**), which was obtained in low yield and characterised by elemental analysis, IR spectroscopy and X-ray crystallography. Analysis by NMR was not possible due to insolubility. High temperature crystallisation of mother-liquor of **1** results in the linkage of two complexes of **1** by coordination of their 'tail' amino groups to a *trans* dichloropalladium(II) unit (Fig. 8). The Pd(II) ions adopt a square-planar coordination environment. The complex exhibits a crystallographically imposed two-fold symmetry, resulting in a somewhat twisted geometry around the *trans*-substituted Pd–N bond with a torsion angle of 76.9(8)° (C5–N3–Pd2–Cl3). The Pd–N and Pd–Cl bond lengths lie within expected ranges for square-planar *cis*- and *trans*-substituted diamino-dichloro palladium(II) complexes.[23,24,30,31] Despite being a neutral polymer, the compression of the chelated Pd(II) centres is close to that observed in the mononuclear dichloropalladium(II) complex **1**.

The complex forms a 1D polymeric chain along the crystallographic c axis with each terminal Pd(II) unit bridging two adjacent molecules *via* Cl ··· H hydrogen bonded interactions. The two pairs of chloro ligands lie *trans* to one another with respect to the Pd–Pd axis (Pd ··· Pd = 3.406(5) Å), see Fig. 9. This is due to hydrogen bonded interactions between the *cis*-chloro ligands and the chelating amino group hydrogens (Cl ··· H = 2.57 and 2.51 Å) positioning them into an eclipsed conformation. This is consistent with observations and theoretical studies on similar compounds by Hambley and co-workers.[32]

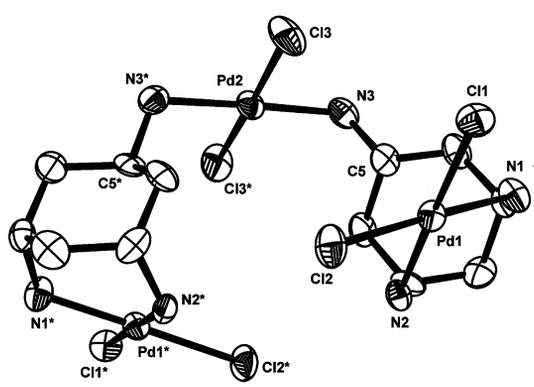

Fig. 8 ORTEP-3 representation of the trinuclear Pd(II) complex [Pd{Pd(**L**)Cl_2}$_2$$Cl_2$] (**7**) at 50% thermal ellipsoids. The twisted geometry can be seen clearly, torsion angle = 76.9(8)° (C5–N3–Pd2–Cl3).

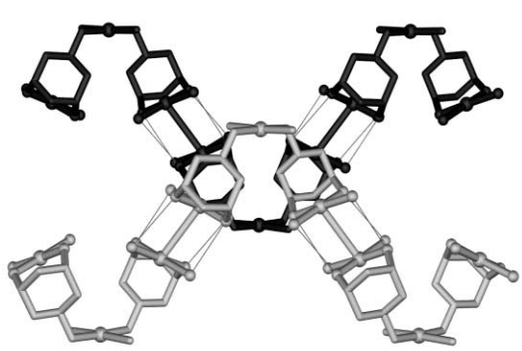

Fig. 9 View along the crystallographic a axis shows two layers of 1D-coordination polymers of **7** along the c axis. Each unit is connected through hydrogen bonded interactions (thin lines connecting small spheres) between chloro ligands and amino group nitrogens. Pd(II) centres are shown as large spheres.

The formation of complex **7** suggests the presence of tetrachloropalladate ions in the mother-liquor of **1** and this assumption is in accordance with the yield increase of the formation of

5 after ion exchange to chloride anions as described above. In addition, tetrabromopalladate ions are observed under similar reaction conditions and starting materials in the formation of complex **2**. Interestingly, the two monoligand Pd(II) units are linked *trans* to each other and not *cis* as would be expected due to *trans*-guiding effects of chloro ligands at nucleophilic substitution reactions on tetrachloropalladate ions.[33] This might be due to steric hindrance for substitutions in *cis* position. In accordance with this, no higher substituted complexes with three or four mononuclear palladium(II) units of **1** around the bridging Pd(II) ion were observed.

Building block approach

The construction of different binding modes of *trans*-tach was achieved by manipulation of the monoligand dichloropalladium(II) complex **1** (Fig. 10). Under a variety of reaction conditions, **1** acts as a building block to facilitate the formation of the different coordination motifs. Strongly alkaline conditions lead to the removal of the chloro ligands of **1** and to the formation of the 'head-to-head' complex **3**. High temperature crystallisation in the presence of tetrachloropalladate ions in the mother-liquor facilitates the formation of the trinuclear 'tail-to-tail' complex **7**. Removal of the tetrachloropalladate ions from the mother-liquor by ion exchange and subsequent neutralisation forms the 'head-to-tail' coordination observed in the hexanuclear metallamacrocycle **5**.[22]

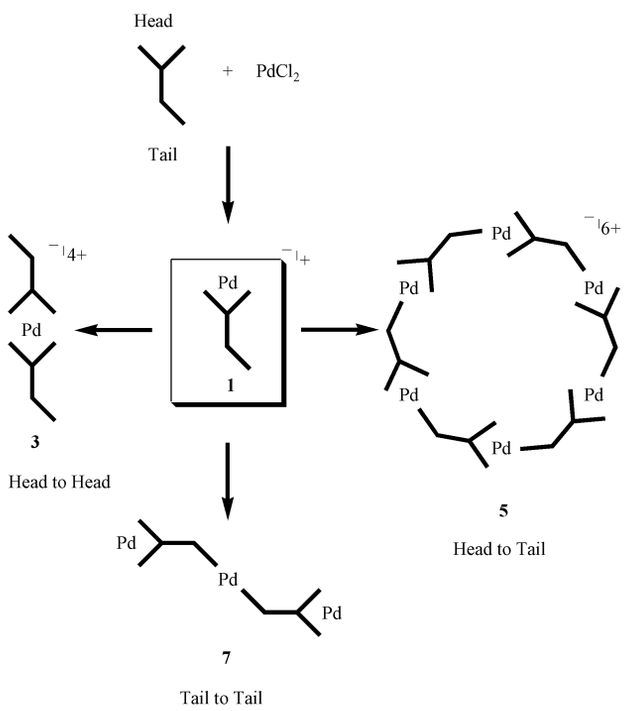

Fig. 10 Reaction of *trans*-tach with palladium(II) chloride results in complex **1** which can further react to form 'head-to-head' complex **3**, 'head-to-tail' complex **5** or 'tail-to-tail' complex **7**. The Pd(II) centres are square planar and the remaining coordination sites are occupied by chloro ligands. In addition to the variety of complexes based on **1**, the monoligand dibromopalladium(II) complex **2** also acts as a building block upon the formation of the hexanuclear 'head-to-tail' complex **6**.

Conclusions

The versatile coordination chemistry of the bimodal ligand *trans*-tach having non-equivalent (bidentate 'head' and monodentate 'tail') and non-interacting (*cis* and *trans*) binding sites with Pd(II) is demonstrated. A variety of coordination compounds with 'head-to-head' (**3**,**4**), 'head-to-tail' (**5**,**6**) and 'tail-to-tail' (**7**) coordination modes were obtained. In addition, the structural flexibility of *trans*-tach in adopting strained conformations was illustrated by variations in the coordinative compression upon 'head' chelation. This work will be extended to other systems involving other metals and derivatives of *trans*-tach.

Experimental

Materials

cis,*trans*-1,3,5-Triaminocyclohexane was synthesised following a known literature procedure.[34] All other reagents were commercially available and used without further purification. ^{1}H and ^{13}C NMR spectra were recorded at room temperature, unless otherwise stated, on a Bruker DRX-500 or DPX-400 spectrometer in D_2O. Infrared spectra were recorded in the range of 4000–750 cm^{-1} on a Shimadzu FTIR-8300 spectrophotometer using a Golden Gate setting for solid material.

Synthesis

$[Pd(LH)Cl_2]Cl$ (1). To an aqueous solution (200 ml) of **L**·3HCl (199 mg, 0.833 mmol) was added $PdCl_2$ (164 mg, 0.925 mmol) and refluxed for two days. The resulting orange solution was concentrated to 20 ml. Orange crystals of **1** were obtained upon standing over 1–2 days at ambient temperature (282 mg, 0.82 mmol, 71% yield). ^{1}H NMR, δ 6.22 (t, 1H, J 13.4 Hz, $C(NH_2)H_{ax}$), 4.27 (br s, NH_2), 2.98 (br s, 2H, $C(NH_2)H_{eq}$), 2.22 (d, 2H, J 13.4 Hz, CH_2-H_{eq}), 2.02 (d, 1H, J 15.3 Hz, CH_2-H_{ax}), 1.75 (td, 2H, J 13.4, 3.2 Hz, CH_2-H_{ax}), 1.60 (d, 1H, J 15.3 Hz, CH_2-H_{eq}). ^{13}C NMR, δ 43.96 ($C(NH_2)H_{eq}$), 43.53 ($C(NH_2)H_{ax}$), 34.14 (CH_2), 33.82 (CH_2). Found: C, 19.67; H, 5.02; N, 11.68. Calc. for $C_6H_{16}N_3Cl_3Pd{\cdot}H_2O$: C, 19.96; H, 5.03; N, 11.64%. IR ν/cm^{-1}: 3368(w), 3209(s), 3117(vs), 2935(s), 1585(s), 1485(s), 1358(m), 1342(s), 1184(vs), 1153(vs), 1045(m), 926(s), 880(m), 718(m), 640(s), 579(s).

$[Pd(LH)Br_2]_2[PdBr_4]$ (2). To an aqueous solution (25 ml) of **L**·3HBr (294 mg, 0.790 mmol) was added $PdBr_2$ (201 mg, 0.755 mmol) and refluxed for two days. The resulting intense orange solution was concentrated to *ca*. 30 ml. Reddish-brown crystals of **2** were obtained upon standing overnight at ambient temperature (185 mg, 0.15 mmol, 40% yield). ^{1}H NMR, δ 6.20 (pt, 1H, J 13.4 Hz, $C(NH_2)H_{ax}$), 3.06 (br s, 2H, $C(NH_2)H_{eq}$), 2.20 (d, 2H, J 13.4 Hz, CH_2-H_{eq}), 2.06 (d, 1H, J 15.6 Hz, CH_2-H_{ax}), 1.76 (td, 2H, J 13.4, 4.0 Hz, CH_2-H_{ax}), 1.65 (br d, 1H, J 15.6 Hz, CH_2-H_{eq}). ^{13}C NMR could not be obtained due to low solubility. Found: C, 11.65; H, 2.63; N, 6.75. Calc. for $C_{12}H_{32}N_6Br_8Pd_3$: C, 11.82; H, 2.65; N, 6.89%. IR ν/cm^{-1} 3434(w), 3180(s), 3099(s), 2894(m), 1560(vs), 1461(vs), 1344(s), 1227(m), 1134(vs), 1041(m), 939(m), 883(s).

$[Pd(LH)_2](NO_3)_4$ (3). (a) An aqueous mother-liquor solution (5 ml) of **1** (21 mg, 0.062 mmol) was adsorbed onto an alkaline ion exchange column in its hydroxide form (Dowex 1X8-50). The alkaline eluent was concentrated and neutralised with nitric acid. Yellowish crystals of **3** were obtained by evaporation over 5–7 days at ambient temperature (16 mg, 0.03 mmol, 74% yield). (b) Alternative route: *trans*-tach (93 mg, 0.723 mmol) and palladium nitrate hydrate (97 mg, 0.421 mmol) were refluxed in water (30 ml) overnight. Crystallisation by evaporation over 5–7 days resulted in 46 mg of **3** (0.075 mmol, 21% yield). ^{1}H NMR, δ 5.38 (tt, 1H, J 13.2, 4.6 Hz, $C(NH_2)H_{ax}$), 3.16 (br s, 2H, $C(NH_2)H_{eq}$), 2.16 (br d, 2H, J 14.3, CH_2-H_{eq}), 1.95 (dt, 1H, J 15.4, 4.1 Hz, CH_2-H_{ax}), 1.82–1.60 (m, 3H, CH_2-H_{eq}, 2 × CH_2-H_{ax}). ^{13}C NMR, δ 44.49 ($C(NH_2)H_{eq}$), 43.38 ($C(NH_2)H_{ax}$), 34.30 (CH_2), 33.98 (CH_2). Found: C, 23.29; H, 5.22; N, 22.66. Calc. for $C_{12}H_{32}N_{10}O_{12}Pd$: C, 23.45; H, 5.25; N, 22.80%. IR ν/cm^{-1}: 3209(s), 3117(vs), 2928(s), 1601(s), 1481(s), 1269(s), 1141(vs), 999(s), 821(s).

$[Pd(LH)_2](SO_4)_2$ (4). To an aqueous solution (20 ml) of *trans*-tach (72 mg, 0.560 mmol) was added $PdSO_4$ (59 mg (0.293

mmol) and refluxed for two days. The pale yellow solution was concentrated to 10 ml. Yellowish crystals of **4** were obtained by evaporation over 14 days at ambient temperature (29 mg, 0.05 mmol, 35% yield). ^{1}H NMR, δ 5.36 (tt, 1H, J 12.7, 4.4 Hz, C(NH$_2$)H_{ax}), 3.12 (br s, 2H, C(NH$_2$)H_{eq}), 2.12 (br d, 2H, J 13.7 Hz, CH$_2$-H_{eq}), 1.89 (dt, 1H, J 15.6, 4.0 Hz, CH$_2$-H_{ax}), 1.70–1.52 (m, 3H, CH$_2$-H_{eq}, 2 × CH$_2$-H_{ax}). ^{13}C NMR, δ 42.65 (C(NH$_2$)-H$_{eq}$), 40.74 (C(NH$_2$)H$_{ax}$), 33.46 (CH$_2$), 32.02 (CH$_2$). Found: C, 25.60; H, 5.72; N, 14.92. Calc. for $C_{12}H_{32}N_6S_2O_8Pd$: C, 25.78; H, 5.77; N, 15.03%. IR ν/cm^{-1}: 3405(br m), 3064(m), 2902(m), 1618(s), 1525(s), 1450(s), 1354(m), 1063(vs), 750(m).

[{Pd(L)Br}$_6$]Br$_6$ (6). To an aqueous solution (300 ml) of **L**·3 HBr (211 mg, 0.57 mmol) was added PdBr$_2$ (402 mg (1.51 mmol) and refluxed for 2 days. The resulting red solution was adsorbed onto an ion exchange resin in its bromide form (Dowex 1 7 × 8–50). The acidic eluent was neutralised with sodium hydroxide. Heating at 50 °C for 5 days resulted in a pale yellow solution which was concentrated to 20 ml. Yellow crystals of **6** were obtained upon standing over a period of 5 days at ambient temperature (50 mg, 0.02 mmol, 22%). ^{1}H NMR (25–65 °C), δ 6.34 (pt, 1H, J 12.7 Hz, H_A), 5.25 (m, 2H, H_B,H_C), 4.34 (br s, NH_2), 4.00 (br s, NH_2), 3.28–2.65 (m, 9H), 2.66 (br d, 1H, J 13.4 Hz, H_D), 2.08–1.86 (m, 5H), 1.70–1.34 (m, 9H). ^{13}C NMR, δ (45.39, 44.85, 44.66, 43.84, 43.40, 43.16, 42.66, 42.10, 9 × CH), (36.99, 36.90, 36.79, 36.16, 36.00, 35.71, 31.75, 31.62, 9 × CH$_2$). Found: C, 13.94; H 5.20; N, 7.78. Calc. for [C$_6$H$_{15}$-Br$_2$N$_3$Pd]$_6$·7H$_2$O: C, 13.82, H 5.60, N 8.06. IR ν/cm^{-1}: 3410(m), 3186(s), 3089(vs), 2924(m), 1576(vs), 1448(w), 1435(w), 1362(s), 1292(w), 1215(m) 1149(m), 1109(m), 1080(w), 1057(s), 1026(m), 928(m), 881(w), 739(bw).

[Pd{Pd(L)Cl$_2$}$_2$Cl$_2$] (7). An aqueous mother-liquor solution (2 ml) of **1** (20 mg, 0.058 mmol) was heated at 80 °C. A small number of orange crystals of **7** were obtained after 7 days (4 mg, 0.01 mmol, 26% yield). NMR spectra could not be obtained due to insolubility in common solvents. Found: C, 18.16; H, 3.98; N, 10.93. Calc. for $C_{12}H_{30}N_6Cl_6Pd_3$: C, 18.24; H, 3.83; N, 10.63%. IR ν/cm^{-1}: 3371(w), 3190(s), 3117(vs), 3228(w), 1701(w), 1570(s), 1512(m), 1362(s), 1339(m), 1223(w), 1184(s), 1153(s), 1049(m), 930(m), 883(w), 718(s).

Crystallography

For crystallographic details see Table 1. Compounds **1** and **7** were measured on a Bruker SMART CCD 6000 [λ(Cu-Kα) = 1.5418 Å]; **2**, **4** and **6** were measured on a Nonius-KappaCCD [λ(Mo-Kα) = 0.7107 Å]; **3** was measured on a Rigaku R-axis [λ(Mo-Kα) = 0.7107 Å]. All diffractometers were equipped with graphite monochromators. Structure solution and refinement with SHELXS-97[35] and SHELXL-97[36] *via* WinGX.[37] Hydrogen atom positions were calculated and subsequently riding. Molecular drawings were generated with ORTEP-3.[38]

CCDC reference numbers 184117 and 214307–214311.

See http://www.rsc.org/suppdata/dt/b3/b307616d/ for crystallographic data in CIF or other electronic format.

References

1 R. E. P. Winpenny, *J. Chem. Soc., Dalton Trans.*, 2002, 1.
2 D. L. Caulder and K. N. Raymond, *Acc. Chem. Res.*, 1999, **32**, 975.
3 D. L. Caulder and K. N. Raymond, *J. Chem. Soc., Dalton Trans.*, 1999, 1185.
4 P. N. W. Baxter, J. M. Lehn, G. Baum and D. Fenske, *Chem. Eur. J.*, 1999, **5**, 102.
5 P. N. W. Baxter, J. M. Lehn, B. O. Kneisel, G. Baum and D. Fenske, *Chem. Eur. J.*, 1999, **5**, 113.
6 R. W. Saalfrank, I. Bernt, E. Uller and F. Hampel, *Angew. Chem., Int. Ed. Engl.*, 1997, **36**, 2482.
7 R. W. Saalfrank, R. Burak, S. Reihs, N. Low, F. Hampel, H. D. Stachel, J. Lentmaier, K. Peters, E. M. Peters and H. G. Vonschnering, *Angew. Chem., Int. Ed. Engl.*, 1995, **34**, 993.
8 F. A. Cotton and G. Wilkinson, *Advanced Inorganic Chemistry*, John Wiley and Sons, New York, 1988.
9 M. Fujita, *Chem. Soc. Rev.*, 1998, **27**, 417.
10 P. M. Stricklen, E. J. Volcko and J. G. Verkade, *J. Am. Chem. Soc.*, 1983, **105**, 2494.
11 P. J. Stang and B. Olenyuk, *Acc. Chem. Res.*, 1997, **30**, 502.
12 B. Olenyuk, A. Fechtenkotter and P. J. Stang, *J. Chem. Soc., Dalton Trans.*, 1998, 1707.
13 M. Fujita and K. Ogura, *Coord. Chem. Rev.*, 1996, **148**, 249.
14 T. Kusukawa and M. Fujita, *Angew. Chem., Int. Ed.*, 1998, **37**, 3142.
15 S. Leininger, B. Olenyuk and P. J. Stang, *Chem. Rev.*, 2000, **100**, 853.
16 M. D. Levin and P. J. Stang, *J. Am. Chem. Soc.*, 2000, **122**, 7428.
17 M. Schweiger, S. R. Seidel, A. M. Arif and P. J. Stang, *Inorg. Chem.*, 2002, **41**, 2556.
18 P. J. Stang, N. E. Persky and J. Manna, *J. Am. Chem. Soc.*, 1997, **119**, 4777.
19 Examples of such, *cis*-blocking ancillary ligands are ethylenediamine, 2,2′-bipyridyl, diphosphinine-BINAP and diphosphininepropane. However, monodentate ligands are also used as blocking units, *i.e.* a variety of sterically demanding phosphinines and chloro ligands.
20 D. A. Beauchamp and S. J. Loeb, *Chem. Commun.*, 2002, 2484.
21 M. J. Hannon, C. L. Painting and W. Errington, *Chem. Commun.*, 1997, 307.
22 G. Seeber, B. Kariuki and L. Cronin, *Chem. Commun.*, 2002, 2912.
23 P. D. Newman, M. B. Hursthouse and K. M. A. Malik, *J. Chem. Soc., Dalton Trans.*, 1999, 599.
24 G. Codina, A. Caubet, C. Lopez, V. Moreno and E. Molins, *Helv. Chim. Acta*, 1999, **82**, 1025.
25 H. J. Callot, J. Fischer and R. Weiss, *J. Am. Chem. Soc.*, 1982, **104**, 1272.
26 T. N. Margulis and L. J. Zompa, *Inorg. Chim. Acta*, 1992, **201**, 61.
27 P. D. Newman, M. B. Hursthouse and K. M. A. Malik, *J. Chem. Soc., Dalton Trans.*, 1999, 599.
28 K. Y. Saito and R., *Chem. Lett.*, 1977, 1141.
29 K. Kamisawa, K. Matsumoto, S. Ooi, H. Kuroya, R. Saito and Y. Kidani, *Bull. Chem. Soc. Jpn.*, 1978, **51**, 2330.
30 Z. Qin, M. C. Jennings and R. J. Puddephatt, *Inorg. Chem.*, 2001, **40**, 6220.
31 M. C. Navarro-Ranninger, M. J. Camazon, A. Alvarezvaldes, J. R. Masaguer, S. Martinezcarrera and S. Garciablanco, *Polyhedron*, 1987, **6**, 1059.
32 R. R. Fenton, F. Huq and T. W. Hambley, *Polyhedron*, 1999, **18**, 2149.
33 A. F. Hollemann and E. Wiberg, *Lehrbuch der Anorganischen Chemie*, Walter de Gruyter, 1995.
34 F. Lions and K. V. Martin, *J. Am. Chem. Soc.*, 1957, **79**, 15721.
35 G. M. Sheldrick, *Acta Crystallogr., Sect. A*, 1998, **46**, 467.
36 G. M. Sheldrick, SHELXL-97. Program for Crystal structure analysis, University of Göttingen, Germany, 1997.
37 L. J. Farrugia, *J. Appl. Crystallogr.*, 1999, **32**, 837.
38 M. N. Burnett and C. K. Johnson, ORTEP-III: Oak Ridge Thermal Ellipsoid Plot Program for Crystal Structure Illustrations, Report ORNL-6895, Oak Ridge National Laboratory, Oak Ridge, TN, USA, 1996.